Neoclassical impurity transport in negative-triangularity plasmas

K. Lim[1*], M. Magal[1], R. Avril[2], Y. Ban[1], C. K. Chai[1], Y. W. Cho[1], G. Dif-Pradalier[3], P. Donnel[3], X. Garbet[1,3], M. Go[1], V. Grandgirard[3], J. Y. Ng[1], K. Obrejan[3], Z. Qu[1], and Y. Sarazin[3]

[1] *School of Physical and Mathematical Sciences, NTU, Singapore*

[2] *Université de Lorraine, CNRS, IJL, France*

[3] *CEA, IRFM, Saint-Paul-lez-Durance, France*

[*] *Speaker e-mail: Kyungtak.lim@ntu.edu.sg*

Introduction

Negative-triangularity plasmas can provide improved confinement without a strong edge pedestal [1]. Their reactor relevance, however, also depends on high-Z impurity control, since neoclassical inward convection can drive tungsten accumulation and enhance core radiation [2]. Although elongation is known to modify impurity poloidal asymmetry and Pfirsch–Schlüter transport [3], the direct role of triangularity remains less established. Here, we derive the dependence of trapped-particle properties, impurity poloidal redistribution, and neoclassical impurity flux on triangularity and elongation. The analytical trends are also assessed using nonlinear global gyrokinetic simulations performed with GYSELA.

Geometry and orbit properties

The flux surfaces are represented using the Miller parameterization [4],

$$R = R_0 + r\cos\left[\theta + \sin^{-1}(\delta)\sin\theta\right], \qquad Z = \kappa r \sin\theta, \tag{1}$$

where δ and κ denote triangularity and elongation. For moderate triangularity, $\sin^{-1}\delta \simeq \delta$, giving $R \simeq R_0 + r\cos(\theta + \delta\sin\theta)$ with an error of order δ^3. Figure 1 shows that the approximation accurately reproduces the original Miller surfaces. Shaping modifies the magnetic-field strength, flux-surface Jacobian, and poloidal magnetic field, thereby affecting trapped-particle dynamics and the geometry-weighted averages entering neoclassical transport.

The effective trapped-particle fraction is evaluated following Ref. [5]. At $\varepsilon = 1/3$, the Miller-geometry results are approximately described by

$$f_\mathrm{t} \simeq 0.75 - 0.08\delta + 0.03(\kappa - 1), \tag{2}$$

showing that negative triangularity increases the trapped-particle fraction, whereas the elongation dependence is comparatively weak.

The banana-orbit width scales as $\Delta_b \sim \rho_L B/B_\mathrm{pol}$, with the circular limit $\Delta_b^\mathrm{circ} \sim q\rho_L/\sqrt{\varepsilon}$. The shaped-geometry dependence is well represented by

$$\frac{\Delta_b}{\Delta_b^\mathrm{circ}} \simeq \kappa^{-1.03}(1-\delta)^{0.15}. \tag{3}$$

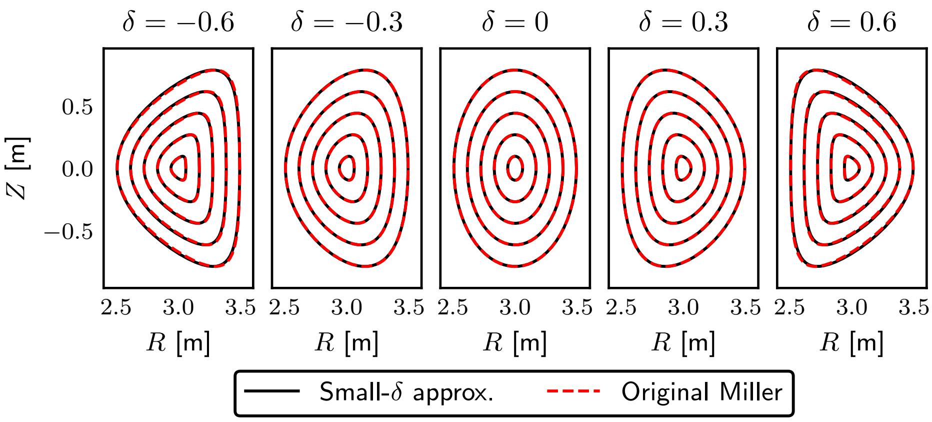

Figure 1: Original Miller surfaces and their small-δ approximation at $\kappa = 1.6$.

Elongation therefore strongly reduces the radial orbit width, whereas negative triangularity produces a weaker broadening. Triangularity primarily modifies the trapped-particle population, while elongation has a stronger influence on radial orbit excursions.

Impurity poloidal asymmetry

For a collisional trace impurity with negligible inertia and viscosity, the parallel force balance is $T_i B \cdot \nabla n_Z = B F_{Zi,\|}$. The leading impurity density variation is represented by

$$\frac{n_Z}{n_{Z0}} = 1 + n_Z^{\mathrm{IO}} \cos\theta + n_Z^{\mathrm{UD}} \sin\theta, \tag{4}$$

where n_Z^{IO} and n_Z^{UD} denote the in–out and up–down asymmetries. The shaping dependence is retained through the weighted moments

$$\mathscr{M}[w] = \int_0^{2\pi} \mathscr{J} w \, d\theta, \qquad \mathscr{N}[w] = \int_0^{2\pi} \frac{\mathscr{J}}{R^2} w \, d\theta. \tag{5}$$

Projection onto the first poloidal harmonics gives

$$n_Z^{\mathrm{UD}} = -\frac{(G/\pi)K_3}{1 + (G/\pi)^2 K_1 K_2}, \qquad n_Z^{\mathrm{IO}} = \frac{G}{\pi} K_1 n_Z^{\mathrm{UD}}, \tag{6}$$

where G is a collisional prefactor and $K_{1,2,3}$ contain the thermodynamic, parallel-flow, and shaped-geometry contributions. Increasing elongation reduces the up–down asymmetry and modifies the in–out redistribution. Triangularity produces a weaker but systematic variation, with negative triangularity generally increasing the magnitude of the up–down component.

Neoclassical impurity flux and GYSELA simulations

The radial impurity flux follows from the toroidal impurity momentum balance,

$$\langle \Gamma_Z^{\mathrm{neo}} \cdot \nabla r \rangle = -\frac{I}{Ze\psi'} \left\langle \frac{F_{Zi,\|}}{B} \right\rangle. \tag{7}$$

Using the parallel force balance and Eq. (6) gives

$$\langle \Gamma_Z^{\mathrm{neo}} \cdot \nabla r \rangle = \frac{I n_{Z0} T_i}{Ze\psi'} \frac{(G/\pi) K_3 C_c}{1 + (G/\pi)^2 K_1 K_2}, \tag{8}$$

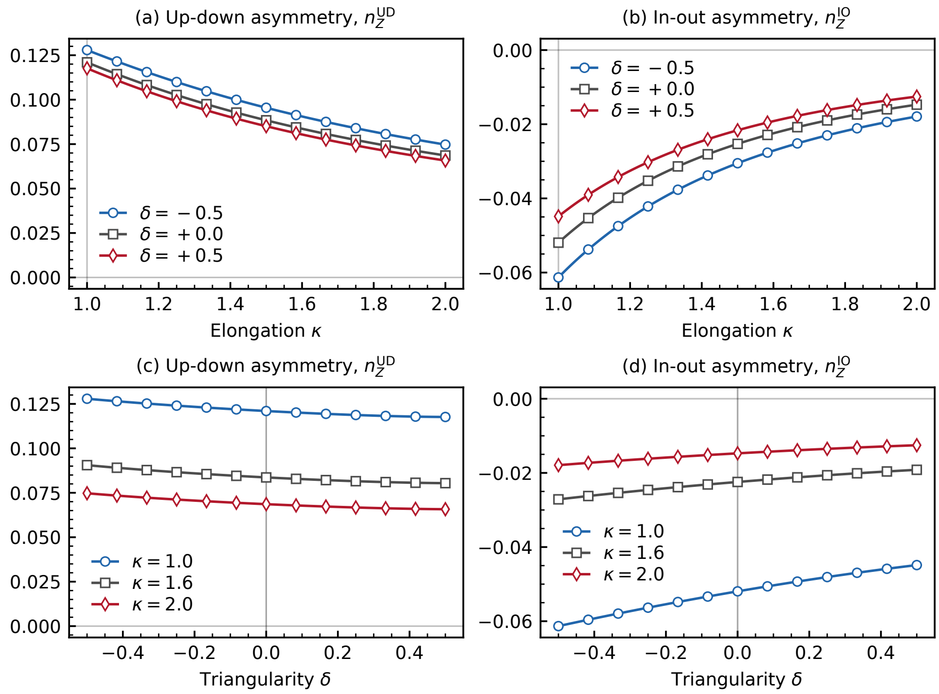

Figure 2: Up–down and in–out impurity asymmetries versus elongation and triangularity.

where C_c is a shape-dependent flux-surface coefficient. Shaping therefore enters through both the magnetic geometry and the impurity poloidal redistribution.

The calculated flux remains inward over the range considered. Increasing elongation substantially reduces its magnitude through the combined reduction of the banana width, up–down asymmetry, and geometry-weighted coefficients. Negative triangularity moderately enhances the inward flux relative to circular and positive-triangularity configurations, although this dependence weakens with increasing aspect ratio.

The analytical trends are assessed using nonlinear, global, full-f, flux-driven gyrokinetic simulations performed with GYSELA [6]. The simulations consider ion-temperature-gradient turbulence with a trace heavy-impurity population, such that the impurity does not modify the background turbulence. The time-averaged heavy-impurity transport remains inward and reproduces the analytical ordering: elongation weakens the inward transport, while negative triangularity produces a moderate enhancement. The simulated impurity poloidal harmonics are also consistent with the dependence predicted by the geometry-weighted coefficients. This agreement indicates that the leading shaping dependence is captured by the impurity poloidal redistribution and associated Pfirsch–Schlüter transport, despite nonlinear turbulence and self-consistent profile evolution.

Conclusions

An analytical description of heavy-impurity transport with explicit triangularity and elongation dependence has been derived. Negative triangularity increases the trapped-particle fraction and moderately broadens banana orbits, whereas elongation strongly reduces the orbit width. Shaping couples the in–out and up–down impurity asymmetries through geometry-weighted moments.

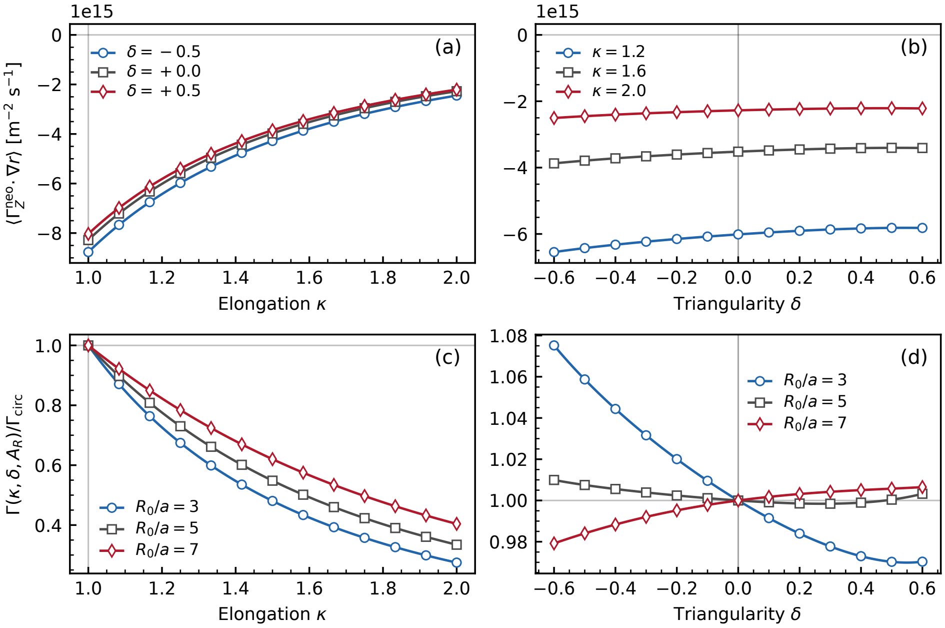

Figure 3: Neoclassical impurity flux versus elongation and triangularity, including normalized scans at different aspect ratios.

The resulting neoclassical flux remains inward. Elongation substantially reduces its magnitude, while negative triangularity produces a weaker enhancement. Nonlinear GYSELA simulations reproduce these trends, showing that the shaping dependence arises primarily through geometry-induced impurity poloidal redistribution and the associated Pfirsch–Schlüter flux.

Acknowledgements

This work was partly supported by the Singapore Ministry of Education Academic Research Fund Tier 1 grants RS38/24 and RG178/25, and by National Research Foundation Singapore core funding for "Fusion Science for Clean Energy" under the Singapore Alliance with France for Fusion Energy. Computational resources were provided by the National Supercomputing Centre, Singapore, under Project 12003525, and by GENCI at TGCC under allocation 2025-A0180502224.

References

[1] A. Marinoni et al., Nucl. Fusion **61**, 116010 (2021).

[2] K. Lim et al., Nucl. Fusion **61**, 046037 (2021).

[3] C. Pan, Nucl. Fusion **63**, 046021 (2023).

[4] R. L. Miller et al., Phys. Plasmas **5**, 973–978 (1998).

[5] F. L. Hinton and R. D. Hazeltine, Rev. Mod. Phys. **48**, 239–308 (1976).

[6] V. Grandgirard et al., Comput. Phys. Commun. **207**, 35–68 (2016).